Integrated System for Bacterial Detection and Biofilm Treatment on Indwelling Urinary Catheters

Ryan C. Huiszoon, Jinjing Han, Sangwook Chu, Justin M. Stine, Luke A. Beardslee, and Reza Ghodssi

***Abstract*—*Goal:* This work introduces an integrated system incorporated seamlessly with a commercial Foley urinary catheter for bacterial growth sensing and biofilm treatment. *Methods:* The system is comprised of flexible, interdigitated electrodes incorporated with a urinary catheter via a 3D-printed insert for impedance sensing and bioelectric effect-based treatment. Each of the functions were wirelessly controlled using a custom application that provides a user-friendly interface for communicating with a custom PCB via Bluetooth to facilitate implementation in practice. *Results:* The integrated catheter system maintains the primary functions of indwelling catheters - urine drainage, balloon inflation - while being capable of detecting the growth of *Escherichia coli*, with an average decrease in impedance of 13.0% after 24 hours, tested in a newly-developed simulated bladder environment. Furthermore, the system enables bioelectric effect-based biofilm reduction, which is performed by applying a low-intensity electric field that increases the susceptibility of biofilm bacteria to antimicrobials, ultimately reducing the required antibiotic dosage. *Conclusion:* Overall, this modified catheter system represents a significant step forward for catheter-associated urinary tract infection (CAUTI) management using device-based approaches, integrating flexible electrodes with an actual Foley catheter along with the control electronics and mobile application. *Significance:* CAUTIs, exacerbated by the emergence of antibiotic-resistant pathogens, represent a significant challenge as one of the most prevalent healthcare-acquired infections. These infections are driven by the colonization of indwelling catheters by bacterial biofilms.**

***Index Terms*—Bacterial biofilm, bioelectric effect, flexible device, impedance sensor, medical implants.**

I. Introduction

CATHETER-associated urinary tract infections (CAUTIs) are one of the most prevalent nosocomial infections, accounting for over 25000 cases in United States' hospitals in 2018, according to the Centers for Disease Control and Prevention (CDC) [1]. The cost burden of CAUTI was estimated to be as high as $450 million in 2007 [2]. CAUTI is driven by the colonization of the catheter by bacterial biofilms [3]. Biofilms are complex structures comprised primarily of exopolysaccharides, extracellular DNA, and bacterial cells, which adhere to hydrated surfaces, particularly on indwelling medical devices [4]. Biofilms are significantly more tolerant of antibiotic therapy than their planktonic counterparts, requiring 500 to 5000 times greater doses for effective treatment [5]. In addition, biofilms can serve as sources of infection, as bacteria can detach from the biofilm and spread the infection [4]. Indwelling urinary catheters are inevitably colonized by biofilm, increasing the risk of developing CAUTI over time [6]. Furthermore, CAUTI can lead to severe complications such as bacteremia, sepsis, and mortality [7], [8].

Guidelines issued by the CDC recommend that indwelling urinary catheters not be changed at routine intervals, but rather based on clinical indications, such as infection or obstruction [9]. However, many clinical indications, such as conventional bacterial cultures, take hours or days to identify potential infections [10]. Furthermore, healthcare practitioners typically wait for symptoms of an infection such as fever, pain, or dysuria to develop before ordering cultures [11]. This time can allow infections to progress significantly; identification of infection risk (i.e., biofilm colonization), leading to prompt catheter removal or treatment, is important for CAUTI management. Several microsensor approaches have been explored to identify biofilm formation in real-time, such as surface acoustic wave [12], optical-density [13], fiber optic sensors [14], and other microsystems [15]. Electrochemical impedance sensors enable continuous biofilm monitoring in a nondestructive manner with relatively low power consumption [16]–[20]. Particularly, flexible impedance sensors have been demonstrated for biofilm monitoring, allowing the detection device to conform seamlessly to a wide range of vulnerable surfaces [21].

Numerous strategies have been explored to reduce the incidence of CAUTI by modifying the surfaces of indwelling catheters. Notably, chemical surface modifications such as impregnation with antiseptics, antibiotics, NO, or metal ions have shown some efficacy in research but have not yet achieved widespread use in clinical practice [22]–[24]. Antibiotic-infused catheters are not desirable, as widespread antibiotic use increases

Manuscript received January 5, 2021; revised February 26, 2021 and March 7, 2021; accepted March 12, 2021. Date of publication March 18, 2021; date of current version October 20, 2021. This work was supported in part by the U.S. National Science Foundation under Grant ECCS1809436, University of Maryland Medical Device Development Fund, and TEDCO Maryland Innovation Innitiative. *(Corresponding author: Reza Ghodssi.)*

Ryan C. Huiszoon, Jinjing Han, Sangwook Chu, Justin M. Stine, and Luke A. Beardslee are with the University of Maryland, USA.

Reza Ghodssi is with the University of Maryland, College Park, MD 20742 USA (e-mail: ghodssi@umd.edu).

This article has supplementary downloadable material available at https://doi.org/10.1109/TBME.2021.3066995, provided by the authors.

Digital Object Identifier 10.1109/TBME.2021.3066995

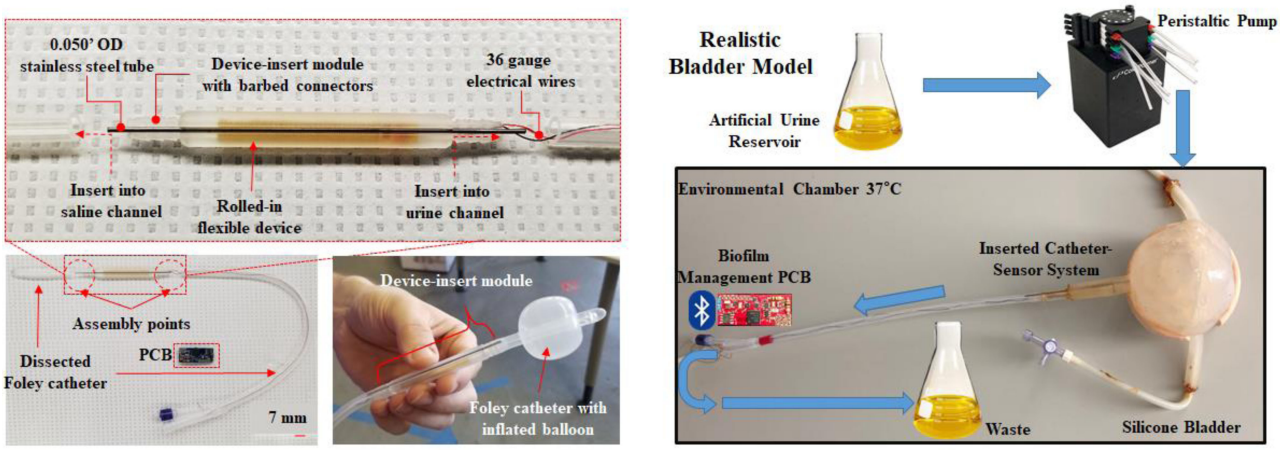

(a) (b)

Fig. 1. Foley catheter insert module and bladder model setup. (a) Components comprising integrated system including steel tube for saline balloon inflation channel, 36 AWG wires to connect PCB with embedded sensor, flexible IDEs, and 3D-printed insert module with barbed connectors for leak proof connection with urine drainage channel. (inset) Optical image of insert module interfaced with 22 Fr Foley catheter with inflated balloon inflated. (b) Overview of realistic bladder model setup.

the risk of selection for antibiotic resistance [11]. To reduce the need for antibiotics, the bioelectric effect (BE) consists of a low intensity electric field in combination with low doses of antimicrobials for synergistic biofilm treatment [25]–[27]. The application of the electric field increases the susceptibility of the biofilm bacteria to antibiotics, decreasing the dosage needed for effective clearance. There are several hypotheses of the mechanism of action for the bioelectric effect. These include increased bacterial membrane permeability, biofilm matrix disruption, electrophoretic augmentation of antimicrobial transport, or electrochemical generation of reactive compounds [28]. In recent years, electrochemical generation of bactericidal compounds such as hypochlorous acid has been used to reduce biofilm formation [29]–[31]. Electric field-based treatment has been demonstrated for a variety of organisms implicated in CAUTI, including *Escherichia coli, Pseudomonas aeruginosa, Klebsiella pneumonia, and Enterobacter sakazakii* [25], [32]–[34].

In this work we present an integrated system for bacterial monitoring and treatment on indwelling Foley catheters. A 3D-printable insert module has been designed to allow integration of interdigitated electrodes (IDEs) with a commercially available urinary catheter without compromising the primary function of Foley catheters for impedance-based, continuous bacterial monitoring in a bladder environment. The IDE based sensor is fabricated on a flexible polyimide substrate and is controlled wirelessly using a custom designed printed circuit board (PCB) and a custom mobile application. Additionally, the IDEs are also used to administer a BE-based treatment, providing a feedback-driven CAUTI management system. The integrated system has strong potential to address challenges of CAUTI by promptly detecting the growth of bacteria to identify catheters that are at risk of developing an infection, ultimately enabling a targeted treatment requiring lower antibiotic dosage in an effective and user-friendly manner. This work represents an important advance over previous work [16], [21] as a fully integrated system incorporated with a standard Foley catheter and a custom PCB for wireless implementation. Furthermore, this integrated system was tested in a newly-developed realistic *in vitro* model of the catheterized bladder.

II. Methods

A. Foley Catheter Insert

A Foley catheter with the integrated insert module is depicted in Fig. 1(a). The device-insert module, comprised of IDEs on the flexible substrate integrated within a 3D-printed insert, allows facile integration at a sliced interface of the commercial urinary Foley catheter via two flow channels - saline and urine channels. The device-insert module was 3D-printed using a Form 2 sterolithography (SLA) 3D printer (FormLabs) using clear resin. As shown in Fig. 1(a), barb structures at the insert tips allowed a robust leak-free connection with the 22 Fr Foley catheter (Bard) urine channels. A stainless steel tube in a groove on the 3D-printed insert module connects the saline balloon inflation channel. A longitudinal groove along the outside wall of the insert accommodated the stainless-steel tube to connect the saline channel for balloon inflation. The insert module is integrated near the distal tip close to the balloon with the sensor on the inner lumen of the urine drainage channel, as this is the area most commonly colonized by biofilm [35]. Biofilm impedance sensing and BE application occur at the inner lumen of the insert urine drainage channel where the flexible electrodes are conformed facing inward. The electrodes can be adapted to be on the outer surface of the catheter in the future. We anticipate that electrodes in contact with the bladder and urethra tissue will not be harmful, as the maximum electric field strength during BE (21.7 V/cm) is well below the threshold for damaging cell viability (100 V/cm) seen in previous work using a similar electrode configuration [36]. The catheter and integrated insert module can be sterilized via autoclave at 121 °C for 20 min. A major design consideration was to maintain the standard urinary Foley catheter configuration when integrating the insert module and associated electronics. This was to assure that the

primary functions of the urinary catheter (urine drainage, bladder anchoring by inflating the balloon at the tip) would be sustained.

The flexible electrodes (20 nm Cr/200 nm Au thick, 300 μm IDE width and spacing) were fabricated on polyimide substrates (25.4 μm thick) via a standard electrode patterning microfabrication technique (lift-off), and the overall device footprint (48 mm $\times$ 10 mm) was adjusted via optical mask design to conform onto the inner lumen of the insert module without any overlap. The fabrication of the flexible electrodes is described in our previous work [21]. This design measures the entire electrochemical cell, including the electrodes, electrolyte, and interface between the two, allowing the sensor to capture the multiple facets indicative of biofilm such as biofilm matrix and changes to the electrolyte due to bacteria metabolism. Furthermore, the interdigitated arrangement possible with a two electrode configuration increases the effective area of the sensor. The 300 μm electrode finger width and spacing was selected as approximately 90% of the electric field is confined within the height of one electrode finger width [37]. This spacing should concentrate the field within the anticipated maximum biofilm thickness on urinary catheters of around 300 μm for focused sensing and treatment [38]. Prior to being rolled into the module, electrical contact leads were established with 36-gauge wires using copper tape, followed by insulation with polyimide tape. The wires run along the inside of the catheter until exiting near the connection for the urine bag and are connected to the PCB.

B. Bladder Model Setup

The modified catheter biofilm management system was evaluated in a synthetic bladder model. Fig. 1(b) depicts the synthetic bladder setup, consisting of a 3D-printed silicone human bladder, the inserted modified catheter system, and artificial urine all maintained at 37 °C in an environmental chamber. This synthetic model recapitulates the biochemical environment for bacterial growth via artificial urine, and the programmable peristaltic pump recapitulates the physical flow conditions found in the catheterized bladder. Utilizing artificial urine promotes bacterial growth that is similar to what is seen in the clinic. This artificial urine media was based on human urine samples and designed to study the growth of urinary pathogens [39]. The growth curve in Figure S1 confirms the growth of *Escherichia coli* K12 W3110 in this artificial urine. This curve was acquired by sampling the $OD_{600\ nm}$ over 24 hours in a 40 ml culture of artificial urine at 37 °C seeded with 1 ml of *Escherichia coli* seeded at $OD_{600\ nm} = 0.050$. The increasing optical density corresponds to increasing growth. A sensor, fabricated as described previously with titanium/gold 10 nm/100 nm, attached to a glass slide and immersed in this solution provided impedance measurements associated with the $OD_{600\ nm}$ to correlate the growth and sensor response (Figure S2).

A 3D-printed silicone model of the human bladder (Lazarus 3D) recreates the physical urine storage/flow system where urinary catheters are inserted. This model has a volume of 350ml, two ureters, and a urethra (Fig. 1C). The device is inserted into the urethra so that urine may drain and the balloon may be inflated. One ureter serves as a valve to drain the bladder at the conclusion of the experiment and the other serves as an inlet to introduce artificial urine at a fixed rate. The tubing connected to the bladder is interfaced with a peristaltic pump that drives the flow. The flow can be maintained at a steady rate, or programmed to flow in intermittent pulses. The bladder with inserted catheter system, tubing, and media reservoirs are autoclaved (20 min, at 121 °C) to ensure sterilization. 500 ml of artificial urine (Table S1) is added to the artificial urine reservoir in a sterile biosafety cabinet. The artificial urine is filtered with a 0.2 μm PES syringe filter to prevent contamination. The complete flow system has ports on both the urine or waste reservoirs with syringe filters to maintain sterility and equalize the pressure during flow experiments. The flow system is placed in an environmental chamber at 37 °C to maintain the temperature and minimize the risk of outside contamination. The pump and urine reservoir are connected to the bladder/catheter system via tygon tubing and stored outside of the environmental chamber. The bladder was left overnight to fill with urine, until the catheter was fully immersed, before growth and treatment experiments were performed.

C. Biofilm Management PCB

The goal of the embedded system development is to leverage the impedance sensing and BE treatment capability presented in our previous work [21] in a realistic environment platform with a user-friendly interface and control system, which can be seamlessly integrated with an indwelling catheter in either a hospital or ambulatory setting. The PCB can be adhered to the external portion of the catheter, connected via 36 AWG wires, and reused. The key specifications for the circuit design include effective implementation of the sensing and treatment signals, small form factor, low power consumption, and the ability to transfer data wirelessly. Furthermore, the system was specifically designed to measure impedances on the order of 102 Ω, which was determined in our previous work [21]. The biofilm management PCB, shown in Fig. 2, contains three critical components: the BGM121 Bluetooth microcontroller (MCU), the AD5933 impedance sensing module, and the AD2S99 sinewave oscillator. The BGM121 MCU is an ideal wireless Bluetooth Low Energy (BLE) solution (Silicon Labs), which contains several energy modes to conserve power, an integrated antenna for efficient RF data transmission, necessary peripheral functions to obtain data, and a robust integrated development environment for MCU programming. This system allowed wireless control over switching between three major modes of operation: Sensing mode with the AD5933, Treatment mode via the AD2S99, as well as a Shutdown mode which consists of both options being switched off for efficient energy use. In Sensing mode, the AD5933 measures the 2 kHz impedance of the electrodes to determine the degree of bacterial growth. In Treatment mode, the AD2S99 generates a 20 kHz sine wave that has been shown to be capable of inducing the BE [33].

Fig. 2 depicts the circuit diagram for the custom PCB. The MCU connects to the AD5933 impedance sensing module via an I2C serial interface. The AD5933 is responsible for generating a frequency sweep across the flexible electrode and digitizing the sensor impedance output for data acquisition. The AD5933 is configured, per the datasheet [34], to measure small impedances

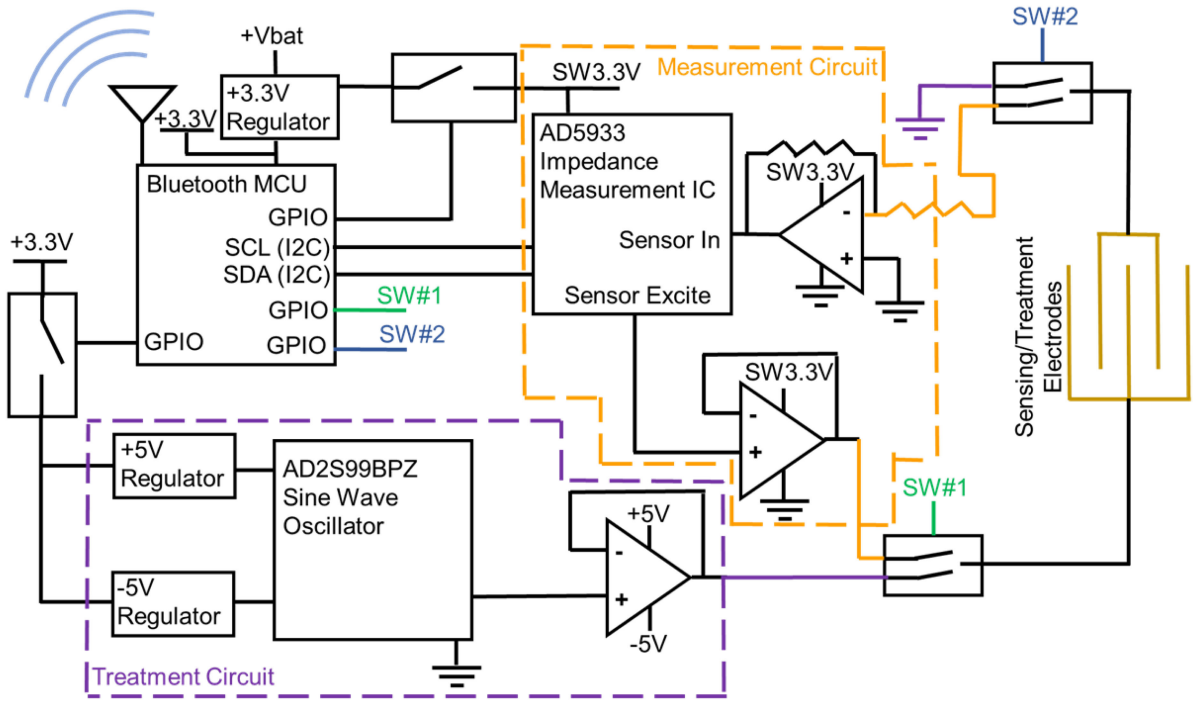

Fig. 2. Circuit diagram for the PCB incorporating Bluetooth MCU, impedance sensing module, and sine wave oscillator for wireless detection and treatment of bacterial biofilms on catheters.

(<1 kΩ) by placing op-amps at the Sensor Excite pin to amplify the excitation signal as well as at the Sensor In pin to properly bias the signal. More specifically, the op-amp, at the AD5933 output, is a non-inverting buffer and the op-amp at the AD5933 input is in an inverting configuration with a gain of 10. For the treatment circuit, the AD2S99 is configured to create a 0.650 Vpk-pk sine wave with a 2.5 V DC offset, which is applied via voltage divider. An op-amp is used as a buffer to source the necessary current to the electrodes instead of sourcing that current through the oscillator. Voltage controlled switches are used to alternate the signals going to the biofilm electrodes between those needed for the AD5933 (sensor in/sensor out) and those needed for the AD2S99 (oscillator output and ground). This fully isolates both circuits from the electrodes when the other circuit is being used. Voltage regulators are used to generate 3.3 V, 5 V, and −5 V, which are needed to drive each of the components. To conserve power, power switches (TPS22810) are used to turn off the power going to either the sensing or treatment circuits when not in use.

The entire circuit is laid out on a 15.5 mm wide by 37 mm long custom four-layer FR-4 PCB. Per the datasheet for the BGM121 [35], specific considerations are required to ensure that the on-package antenna can operate efficiently in order to transmit the Bluetooth signal. Major considerations for the board layout that directly relate to propagation distance are the placement of the chip (i.e., centered with the edge where the antenna is located next to the board edge) and the ground plane clearance areas in the board layers surrounding the antenna (to avoid shorting the antenna). Taking these considerations into account, the board is efficiently able to transmit a Bluetooth signal to a smartphone at a distance of at least 40 meters within a hallway in our laboratory building (Figure S3).

D. Impedance Sensing Algorithm

The I^2C interface is used to program the AD5933 per the datasheet [40] and to read the data stored within the device. A frequency sweep is used to obtain the necessary impedance data, with the measured impedance value recorded at 2 kHz. This was selected as the lowest frequency that could reliably be measured using the AD5933. Briefly, commands formatted as 8-bit words are sent to the AD5933 in the following sequence to initiate a frequency sweep. (1) The start frequency, number of frequency increments and the frequency increment are programmed, (2) the AD5933 is placed in standby mode, (3) the AD5933 is initialized with a start frequency command, (4) the start frequency sweep command is sent after a specified settling time, (5) the MCU then polls a status register to see if the frequency data is present, (6) if data is present the impedance value is read from the AD5933, (7) the MCU polls the status register to see if the frequency sweep is complete, (8) if it is not complete the frequency is incremented and the measurement is repeated starting with step (5), and if the frequency sweep is complete the AD5933 powers down. A key consideration for the impedance measurement circuit is the calibration of the AD5933. This is accomplished using resistors with known impedance values, as described in the AD5933 datasheet [40].

E. Biofilm Management Mobile Application

To operate the system, a custom, user-friendly mobile application was developed to wirelessly control the PCB and export and display data. The application has both iOS and Android compatible versions and is designed to send commands to the PCB to transition between Sensing, Treatment, and Shutdown modes. In addition, the application reads the raw values from

the AD5933 and displays the calculated impedance. Figure S4 depicts each of the screens of the application. The application also displays whether the impedance values have surpassed a threshold value that is set by the user to indicate bacterial growth. Overall, this application allows user-friendly control which facilitates widespread implementation of this tool in research and clinical settings.

After pairing with a device, the device details are shown via a dropdown menu of commands that can be sent to the device, including, Take Measurement, Initiate Treatment, Shutdown, Set Threshold, and Set Gain, summarized and shown in Figure S4. Take Measurement begins the impedance sensing, Initiate Treatment prompts the system to output a sine wave for treatment, Shutdown turns off all functions to save power, Set Threshold determines a relative change in impedance which will trigger a notification in the application, and Set Gain sets the gain factor used to calibrate the sensor via the process described in the AD5933 datasheet [40].

Updates to the measurement parameters, impedance values, and connecting and disconnecting events, are recorded in the activity log on the device details screen. This screen also indicates whether the impedance has surpassed the threshold set by the user. The chart icon will display a chart depicting all of the recorded measurements over time for the currently connected device. When in the pairing screen, the export data feature allows all of the data contained in the activity log to be exported in a spreadsheet. This includes the type of command, impedance data, raw values, time stamps, and device names.

F. Impedance Sensing Characterization

Detection experiments were performed using the aforementioned bladder model at 37 °C (Section V.2). With the bladder and catheter full of artificial urine flowing at 7 ml/h, an initial measurement at t = 0 is taken using the mobile application. This initial measurement serves as the reference point for the relative percent change in impedance. Then, 1ml of *Escherichia coli* K12 W3110 at a dilution of $OD_{600\ nm} = 0.05$ were added to the system, corresponding to 8.9×10^6 CFU/ml. This strain is an effective biofilm former [41]. The bacterial culture was prepared in 5 ml of artificial urine and cultured overnight (37 °C, 120 rpm) in an incubator shaker (Brunswick Instruments). A 1:100 dilution of this culture was then grown overnight and diluted relative to artificial urine without any bacteria added. Control samples were made without any bacteria added and 10 μg/ml gentamicin to ensure that there was no contamination throughout the experiment. Continuous measurement of the impedance was performed every 30 min throughout the growth period. The change in impedance was recorded as a percentage relative to the initial impedance value, to account for small discrepancies between the starting raw impedance values of different sensors. An end-point impedance value was recorded after 24 hours of growth. The adhered biomass was determined using a crystal violet absorbance assay at the conclusion of the pulsatile flow experiment. This consisted of filling the catheter and insert completely with 0.1% crystal violet solution. The crystal violet binds with the biofilm material on the surface of the catheter and insert for 15 min. The solution was then drained from the catheter and the system is then rinsed with 10 ml of deionized water to remove excess stain. The insert is carefully removed from the catheter and immersed in 35 ml of decomplexation solution (1 acetone: 4 ethanol). The decomplexation solution dissolves the bound stain (30 min constant flow, 35 min pulsatile flow). The $OD_{590\ nm}$ of the resulting solution corresponds to the relative biomass adhered on the insert with and without biofilm. The negative control measurement ($OD_{590\ nm} = 0.261 \pm 0.024$ for constant flow, $OD_{590\ nm} = 0.239 \pm 0.008$ for pulsatile flow) served as a baseline; the baseline signal is driven by precipitates which form in the artificial urine media at 37 °C [39]. The baseline was subtracted from each measurement to isolate the contribution due to biofilm growth. In addition, the sensor response was correlated with bacterial growth by incubating the sensor in a beaker with 80 ml of filtered artificial urine at 37 °C. The change in $OD_{600\ nm}$ due to growth was related to the decrease in impedance in Figure S2.

G. BE Treatment

After this growth period, one of four different conditions were set for the treatment period: (1) no additional treatment (untreated), (2) 10 μg/ml gentamicin and continuous 650 mV, 20 kHz AC signal (BE), (3) 10 μg/ml gentamicin (antibiotic-only), and (4) continuous 650 mV, 20 kHz AC signal (electric field-only). Gentamicin was added to the artificial urine media reservoir to achieve the 10 μg/ml concentration. The unseeded negative control received no additional treatment. After the treatments had been applied for 24 hours under constant flow conditions (7 ml/h), the end-point impedance was measured using the mobile application and recorded relative to the impedance at the start of the treatment period. At each end-point, the planktonic cell counts were recorded by taking approximately 0.5 ml from the outlet, performing a serial dilution, and counting the CFU/ml on agar plates. The adhered biomass was determined using a crystal violet absorbance assay (Section V.6). The $OD_{590\ nm}$ of the resulting solution corresponds to the relative biomass adhered on the insert for each of the treatment conditions, to determine the efficacy with regards to biofilm reduction. One-way ANOVA was performed to evaluate the significance of the impedance sensing and biofilm treatment biomass and CFU/ml results.

III. Results and Discussion

A. System Integration With Foley Catheters

The integrated system displayed appropriate liquid drainage from the bladder through the normally inserted catheter without any leakage, draining water at a rate of 2.5 ml/min over four hours (Figure S5). The flow dynamics are not expected to change as the shape and dimensions of the urine drainage channel in the insert match those of the 22 Fr Foley catheter. In addition, this system enabled inflation of the anchoring balloon, demonstrating that the intended function of the catheter is maintained (Figure S6). This approach allows not only unimpeded

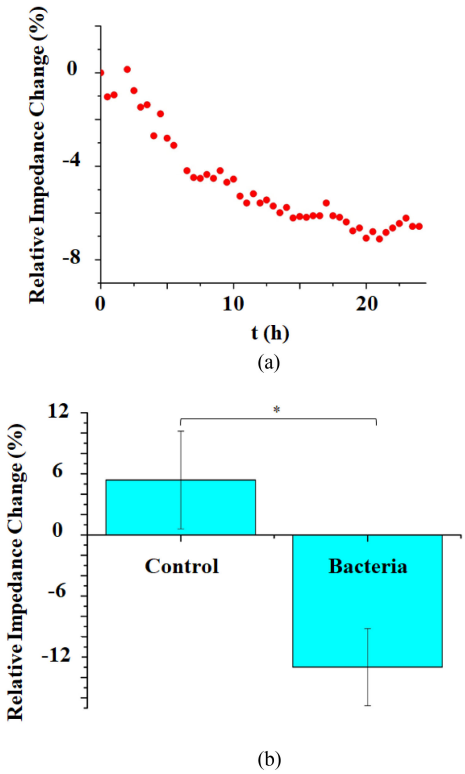

Fig. 3. (a) Representative real-time relative change in 2 kHz impedance showing decrease during bacterial growth. (b) End-point relative change in impedance after 24 hours of growth. Control N = 3, Bacteria N = 8, *Significance $P < 0.05$.

functionality of the Foley catheter, but also biofilm management via the integrated system.

B. Impedance Sensing Under Constant Flow

Fig. 3(a) is a representative plot of the impedance change recorded every 30-minutes for 24 hours with *Escherichia coli* K12 W3110 added under constant artificial urine flow of 7 ml/h using the bladder model. *Escherichia coli* are the most common pathogen isolated in CAUTI [42]. For this reason, this strain will serve as a demonstration for this system. However, testing this system with other species or isolates involved in CAUTI such as *Pseudomonas aeruginosa* and *Proteus mirabilis* is essential future work [43], [44]. The sensor does not incorporate any biorecognition elements that confer specificity for certain bacterial species and is a general growth sensor. The impedance decrease is initially more rapid immediately following the addition of the bacteria at t = 0, and then slows after the first 6.5 hours. The impedance decreases by approximately 4.2% relative to the initial baseline measurement over the first 6.5 hours for a rate of −0.65%/h. The decrease then slows, decreasing an additional 2.4% over the next 17.5 hours for a rate of −0.14%/h. This parallels the growth of the bacteria, with a rapid exponential growth phase followed by a plateau [45]. The growth pattern also matches the sensor response seen in previous work with this type of sensor [16], [21]. The end-point impedance sensing results show a 13.0% decrease when bacteria are added versus a 5.4% increase for the negative control (Fig. 3(b)), demonstrating the viability of this system as a detection tool for the presence of bacteria on an inserted urinary catheter in an artificial urine environment. This trend is similar to what was seen in previous work in standard Luria Bertani broth media [21]; the reduced magnitude and rate of the impedance change in this work is attributed to the lower concentration of nutrients in artificial urine, leading to decreased bacterial growth. The decrease in impedance at 2 kHz seen in Fig. 2 arises due to the increased capacitance of biofilm along with cells and artificial urine compared to artificial urine alone [46]. The following (1) describes the relationship between the impedance and the frequency (ω), resistance of the bulk solution (R_{Sol}), the resistance of biofilm formed on the surface (R_{bio}), the interfacial capacitance (C_{dl}), and the capacitance of the biofilm on the surface (C_{bio}).

$$Z = Rsol + Rbio + \frac{2}{j\omega Cdl} + \frac{1}{j\omega Cbio} \quad (1)$$

The slight increase seen in the bacteria-free negative control is due to the formation of small bubbles on the sensor surface over time, as the artificial urine media is stored at an elevated temperature [39]. The bubbles do not interact with the surface when bacteria are present due to a layer of biofilm forming on the surface. Relative impedance change is correlated with bacterial growth in artificial urine in Figure S2. This indicates that the increasing bacterial concentration in artificial urine is correlated with decreasing impedance values throughout the growth period. It is important to recognize that this sensor provides only a single value for the entire device footprint. Biofilm growth is very heterogeneous, and in future iterations of this device sensor arrays will be explored to achieve better spatial resolution to understand this heterogeneity. This approach will also help explore the contributions of biofilm thickness versus surface coverage.

C. Impedance Sensing Under Pulsatile Flow

The synthetic bladder model can be utilized to recreate both the biochemical and physical characteristics of the catheterized bladder. Fig. 4(a) presents a sample of the impedance recorded every 30 minutes for 10 hours while the sample was subjected to a pulsatile flow pattern which mimics periodic filling of the bladder, followed by catheter drainage. Pulsatile flow consisted of 21 ml flowed every three hours in a pulse with a flow rate of 5 ml/min, allowing the system to be evaluated under realistic and variable flow conditions. The electrodes are immersed in artificial urine for the duration of the experiment. The sample initially displays some variability in the impedance change, which is attributed to the lack of a significant biofilm on the surface and inconsistent growth stemming from the static flow between drainage events. Over time, however, the signal becomes more consistent. The impedance decreases approximately 10.8% over this 10-hour period. The end-point results in Fig. 4(b) display the relative change in impedance after 24 hours of pulsatile flow. The relative decrease in impedance of approximately 20.0% for the samples with bacterial growth compared to a 4.3% increase for the negative control confirms that this system reliably functions as an impedance sensor for monitoring bacterial growth in urinary catheters under realistic flow conditions. The crystal violet

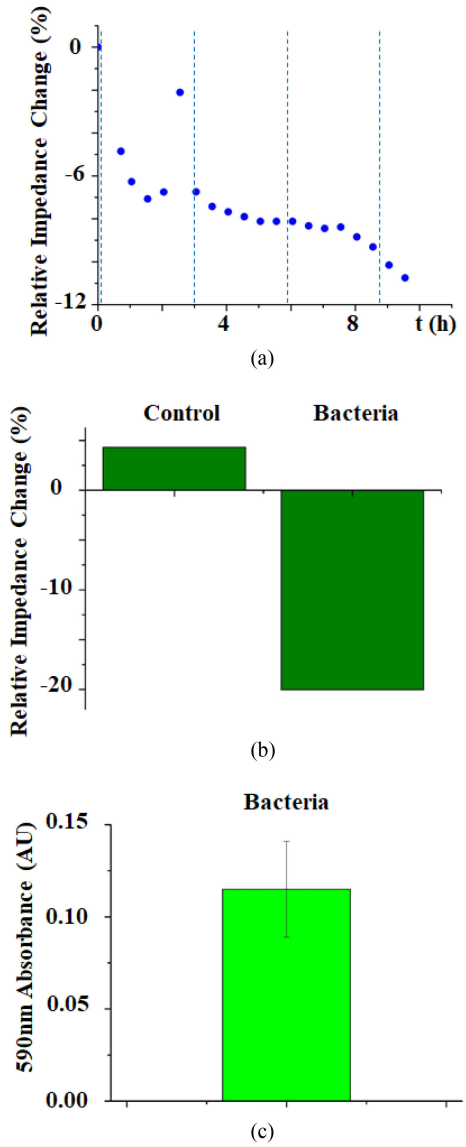

Fig. 4. (a) Real-time 2 kHz relative change in impedance showing decrease with bacterial growth under pulsatile flow conditions. Dashed blue lines correspond to flow pulses. (b) End-point relative change in impedance for bacterial growth and control samples under pulsatile flow. (c) Biomass quantification with bacteria relative to unseeded samples under pulsatile flow, showing a correlation between increased biomass and decreasing impedance (N = 2).

absorbance assay adhered biomass measurements in Fig. 4(c) further corroborate this implication, demonstrating a correlation between the impedance decrease and an increase in biofilm growth. These results imply that the system functionality is maintained under variable and realistic flow patterns that may be found in the catheterized bladder. The impedance change and biofilm growth show similar trends in both pulsatile and constant flow cases. Some research suggests that increased shear may contribute to thicker and increased biofilm growth [47]. However, future work with more samples and additional flow rates and patterns is needed to verify this relationship with this system. This type of study has been made possible by the system developed in this work.

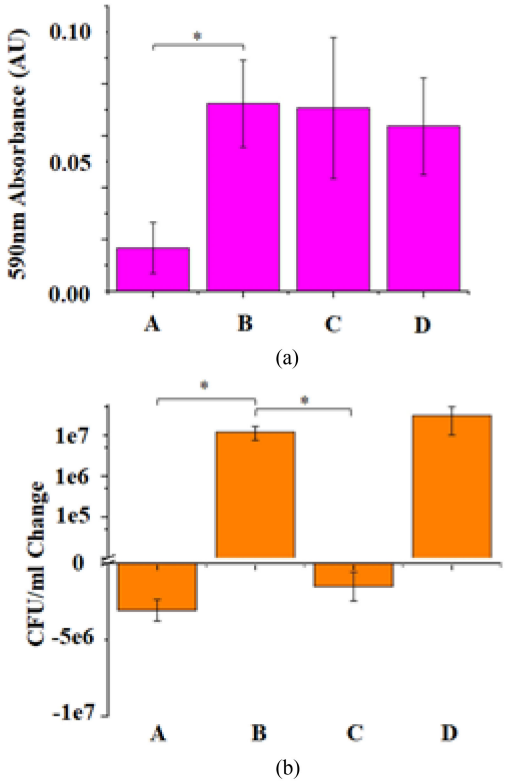

Fig. 5. (a) End-point biomass staining corresponding to each treatment after the 24-hour treatment period and (b) the change in CFU/ml for each treatment during this period. This shows the lowest biomass for the BE treatment, as well as the largest decrease in CFU/ml. A- BE treated samples (N = 3 (a), N = 3 (b)), B- untreated samples (N = 3 (a), N = 3 (b)), C- gentamicin-only treated samples (N = 3 (a), N = 3 (b)), and D- electric field-only treated samples (N = 3 (a), N = 3 (b)). *Significance $P < 0.05$.

D. Biofilm BE Treatment Characterization

Following the growth of bacteria in the catheterized bladder model for 24 hours, this system enables BE-based treatment to remove biofilms adhered to the catheter surface. The BE treatment kills constituent cells in the biofilm more effectively, preventing further proliferation and promoting biofilm removal relative to other treatments. The resulting biofilm biomass at the end of 24 hours of treatment was evaluated using a crystal violet absorbance assay and plotted using the $OD_{590\ nm}$ of the unseeded control as a baseline in Fig. 5(a), showing highest optical density for untreated samples ($OD_{590\ nm} = 0.072 \pm 0.017$). This degree of biofilm formation was comparable to those samples treated with gentamicin-only or electric field-only ($OD_{590\ nm} = 0.071 \pm 0.027$ and $OD_{590\ nm} = 0.064 \pm 0.025$, respectively). This result for biofilm in artificial urine is consistent with previous *in vitro* results demonstrating that an electric field with this intensity or gentamicin at this concentration has limited efficacy for biofilm reduction [21]. Furthermore, the BE showed significantly ($P < 0.05$) lower biomass ($OD_{590\ nm} = 0.017 \pm 0.010$) than the untreated samples, displaying a synergistic reduction in biofilm using this system. This contrasts with the relative ineffectiveness of the gentamicin and electric field treatments for reducing biofilm. It should be

noted that the biomass quantification focused on the sensor insert where the electric field was present. The efficacy of this approach would likely improve by having the electrodes act on a higher percentage of the vulnerable surface.

In addition to biofilm biomass evaluation, the change in CFU/ml during each of these treatments was also examined in Fig. 5(b). Expectedly, the planktonic bacterial counts rose significantly over the 24 hours of treatment for untreated samples. Similarly, the electric field-treated samples showed an increase in bacterial cells comparable to the untreated control, as the electric field only acts on a small portion of the catheter surface, and is shown to have limited impact on cell viability [25]. Gentamicin-only shows a significant ($P < 0.05$) decrease in planktonic cells relative to the untreated samples, as these cells are not as tolerant of antibiotic therapy as cells in a biofilm are. The BE shows the most significant ($P < 0.05$) reduction in planktonic cells relative to the untreated samples, owing to the combined impact of the antibiotic on the planktonic cells and the synergistic impact of the electric field and gentamicin on the biofilm on the insert surface. It is essential to address both surface-associated and planktonic bacterial growth when developing tools for CAUTI management. These results, in combination, demonstrate this integrated system as a viable approach for applying the BE in the catheterized bladder environment and reducing the impact of *Escherichia coli* infection.

IV. Conclusion

The integrated bacteria/biofilm management system developed in this work provides a potentially clinically-viable solution for the management of CAUTI. The system integrates impedimetric sensing and BE treatment seamlessly with the commercially available urinary catheter, allowing this prototype to be readily incorporated into clinical practice. Furthermore, the custom PCB and mobile application enable user-friendly wireless control and user-friendly data transmission. This integrated system will facilitate the translation of this approach to clinical settings. The performance of both the sensing and treatment was evaluated in a realistic *in vitro* bladder model, demonstrating the viability of this approach for future *in vivo* studies. A decrease of 13.0% in relative impedance was seen with the addition of bacteria, compared to a 5.4% increase for the negative control, following the expected trend observed from previous works [16], [21]. The strong correlation between the decrease in impedance with bacterial growth and increasing biofilm biomass demonstrates the potential for real-time indication of infection risk. Effective infection management involves both prompt detection and treatment, which reduces reliance on antibiotics. In this case we demonstrated the BE treatment in the bladder model, showing reduced biofilm on the device surface while using only a minimal antibiotic dosage to help reduce the spread of antibiotic resistance while managing CAUTI. Subsequent studies will focus on testing this system *in vivo* and in clinical settings, as well as incorporating sensors for additional CAUTI biomarkers. The electrode device design can be modified to cover the other vulnerable surfaces of the catheter, such as the outer lumen. Other aspects such as safety and long-term stability should also be explored in the future to further establish utility in clinical settings. Furthermore, this sensing-treatment system for biofilm-based infection management is widely applicable for other areas that are vulnerable to bacterial infections, including prosthetic implants and water systems.

Acknowledgment

The authors would like to thank the Maryland Nanocenter and its FabLab for cleanroom facility support, Harbor Designs and Manufacturing for insert design support, and John Hadeed and JMH Technologies for software development support.

References

[1] C. for D. C. and P. N. C. for E. Z. I. Diseases, "2018 National and state healthcare-associated infections progress report," pp. 1–13, 2019.
[2] R. D. Scott, "The direct medical costs of healthcare-associated infections in U.S. hospitals and the benefits of prevention," pp. 1–13, Mar. 2009.
[3] N. Sabir *et al.*, "Bacterial biofilm-based catheter-associated urinary tract infections: Causative pathogens and antibiotic resistance," *Amer. J. Infect. Control*, vol. 45, no. 10, pp. 1101–1105, 2017.
[4] J. W. Costerton, P. S. Stewart, and E. P. Greenberg, "Bacterial biofilms: A common cause of persistent infections," *Science*, vol. 284, no. 5418, pp. 1318–1322, 1999.
[5] H. Anwar, M. K. Dasgupta, and J. W. Costerton, "Testing the susceptibility of bacteria in biofilms to antibacterial agents," *Antimicrob. Agents Chemother.*, vol. 34, no. 11, pp. 2043–2046, 1990.
[6] J. W. Warren, "Catheter-associated urinary tract infections," *Int. J. Antimicrob. Agents*, vol. 17, no. 4, pp. 299–303, 2001.
[7] P. W. Smith and J. M. Mylotte, "Nursing home-acquired bloodstream infection," *Infect. Control Hosp. Epidemiol.*, vol. 26, no. 10, pp. 833–837, 2005.
[8] C. S. Hollenbeak and A. L. Schilling, "The attributable cost of catheter-associated urinary tract infections in the United States: A systematic review," *Amer. J. Infect. Control*, vol. 46, no. 7, pp. 751–757, 2018.
[9] C. V. Gould, *et al.*, "Guideline for prevention of catheter-associated urinary tract infections 2009 guideline for prevention of catheter-associated urinary tract infections 2009," *Infect. Control Pract. Advis. Comm. Sour Infect. Control Hosp. Epidemiol.*, vol. 31, no. 4, pp. 319–326, 2010.
[10] D. G. Maki, C. E. Weise, and H. W. Sarafin, "A semiquantitative culture method for identifying intravenous-catheter-related infection," *N. Engl. J. Med.*, vol. 296, no. 23, pp. 1305–1309, 1977.
[11] T. M. Hooton *et al.*, "Diagnosis, prevention, and treatment of catheter-associated urinary tract infection in adults: 2009 international clinical practice guidelines from the infectious diseases society of america," *Clin. Infect. Dis.*, vol. 50, no. 5, pp. 625–663, 2010.
[12] Y. W. Kim *et al.*, "An ALD aluminum oxide passivated surface acoustic wave sensor for early biofilm detection," *Sensors Actuators, B. Chem.,* vol. 163, no. 1, pp. 136–145, 2012.
[13] M. T. Meyer, *et al.*, "Development and validation of a microfluidic reactor for biofilm monitoring via optical methods," *J. Micromechanics Microeng.*, vol. 21, no. 5, 2011, Art no. 54023.
[14] Y. Yuan *et al.*, "Electrochemical surface plasmon resonance fiber-optic sensor: In situ detection of electroactive biofilms," *Anal. Chem.*, vol. 88, no. 15, pp. 7609–7616, 2016.
[15] S. Subramanian, *et al.*, "Microsystems for biofilm characterization and sensing – A review," vol. 2, 2019, Art. no. 100015.
[16] S. Subramanian, *et al.*, "An integrated microsystem for real-time detection and threshold-activated treatment of bacterial biofilms," *ACS Appl. Mater. Interfaces*, p. acsami.7b04828, 2017.
[17] J. Paredes, *et al.*, "Real time monitoring of the impedance characteristics of Staphylococcal bacterial biofilm cultures with a modified CDC reactor system," *Biosens. Bioelectron.*, vol. 38, no. 1, pp. 226–232, 2012.
[18] J. Paredes, S. Becerro, and S. Arana, "Label-free interdigitated microelectrode based biosensors for bacterial biofilm growth monitoring using Petri dishes," *J. Microbiol. Methods*, vol. 100, no. 1, pp. 77–83, 2014.
[19] L. Liu *et al.*, "Monitoring of bacteria biofilms forming process by in-situ impedimetric biosensor chip," *Biosens. Bioelectron.*, vol. 112, pp. 86–92, 2018.
[20] I. Tubia, *et al.*, "Sensors and actuators A: Physical Brettanomyces bruxellensis growth detection using interdigitated microelectrode based sensors by means of impedance analysis," *Sensors Actuators A. Phys.*, vol. 269, pp. 175–181, 2018.

[21] R. C. Huiszoon *et al.*, "Flexible platform for in situ impedimetric detection and bioelectric effect treatment of escherichia coli biofilms," *IEEE Trans. Biomed. Eng.*, vol. 66, no. 5, pp. 1337–1345, 2018.
[22] B. W. Trautner, R. A. Hull, and R. O. Darouiche, "Prevention of catheter-associated urinary tract infection," *Curr. Opin. Infect. Dis.*, vol. 18, no. 1. pp. 37–41, 2005.
[23] K. D. Mandakhalikar, R. R. Chua, and P. A. Tambyah, "New technologies for prevention of catheter associated urinary tract infection," *Curr. Treat. Options Infect. Dis.*, vol. 8, no. 1, pp. 24–41, 2016.
[24] A. Colletta *et al.*, "S-Nitroso-N-acetylpenicillamine (SNAP) impregnated silicone foley catheters: A potential biomaterial/device to prevent catheter-associated urinary tract infections," *ACS Biomater. Sci. Eng.*, vol. 1, no. 6, pp. 416–424, 2015.
[25] J. W. Costerton, *et al.*, "Mechanism of electrical enhancement of efficacy of antibiotics in killing biofilm bacteria," *Antimicrob. Agents Chemother.*, vol. 38, no. 12, pp. 2803–2809, 1994.
[26] A. E. Khoury, *et al.*, "Prevention and control of bacterial infections associated with medical devices," *ASAIO J.,* vol. 38, no. 3, 1992, Art. no. M174.8.
[27] J. L. Del Pozo, M. S. Rouse, and R. Patel, "Bioelectric effect and bacterial biofilms. A systematic review," *Int. J. Artif. Organs*, vol. 31, no. 9, pp. 786–795, 2008.
[28] J. L. del Pozo, M. S. Rouse, and R. Patel, "Bioelectric effect and bacterial biofilms. A systematic review," *Int. J. Artif. Organs*, vol. 31, no. 9. pp. 786–795, 2008.
[29] M. M. Kiamco *et al.*, "Hypochlorous-acid-generating electrochemical scaffold for treatment of wound Biofilms," *Sci. Rep.*, vol. 9, no. 1, pp. 1–13, 2019.
[30] V. Lochab *et al.*, "Ultrastructure imaging of Pseudomonas Aeruginosa lawn biofilms and eradication of the tobramycin-resistant variants under in vitro electroceutical treatment," *Sci. Rep.*, vol. 10, no. 1, pp. 1–12, 2020.
[31] D. H. Dusane *et al.*, "Electroceutical treatment of pseudomonas aeruginosa biofilms," *Sci. Rep.*, vol. 9, no. 1, pp. 1–13, 2019.
[32] Y. W. Kim *et al.*, "Effect of electrical energy on the efficacy of biofilm treatment using the bioelectric effect," *NPJ Biofilms Microbiomes*, vol. 1, no. 1, July., 2015, Art. no. 15016.
[33] P. Stoodley, D. DeBeer, and H. M. Lappin-Scott, "Influence of electric fields and pH on biofilm structure as related to the bioelectric effect," *Antimicrob. Agents Chemother.*, vol. 41, no. 9, pp. 1876–1879, 1997.
[34] M. C. P. Pérez, *et al.*, "Inactivation of Enterobacter sakazakii by pulsed electric field in buffered peptone water and infant formula milk," *Int. Dairy J.*, vol. 17, no. 12, pp. 1441–1449, 2007.
[35] G. T. Werneburg *et al.*, "The natural history and composition of urinary catheter biofilms: Early uropathogen colonization with intraluminal and distal predominance," *J. Urol.*, vol. 203, no. 2, pp. 357–364, 2020.
[36] S. D. McCullen, *et al.*, "Application of low-frequency alternating current electric fields via interdigitated electrodes: Effects on cellular viability, cytoplasmic," *Tissue Eng. Part C.*, no. 6, pp. 1–10, 2010.
[37] P. Van Gerwen *et al.*, "Nanoscaled interdigitated electrode arrays for biochemical sensors," *Sensors Actuators, B. Chem.,* vol. 49, no. 1/2, pp. 73–80, 1998.
[38] L. Ganderton, *et al.*, "Scanning electron microscopy of bacterial biofilms on indwelling bladder catheters," *Eur. J. Clin. Microbiol. Infect. Dis.*, vol. 11, no. 9, pp. 789–796, 1992.
[39] T. Brooks and C. W. W. Keevil, "A simple artificial urine for the growth of urinary pathogens," *Lett. Appl. Microbiol.*, vol. 24, no. 3, pp. 203–206, 1997.
[40] A. Devices, "AD5933 material safety data sheet," pp. 40, 2005.
[41] P. N. Danese, L. A. Pratt, and R. Kolter, "Exopolysaccharide production is required for development of Escherichia coli K-12 biofilm architecture," *J. Bacteriol.*, vol. 182, no. 12, pp. 3593–3596, 2000.
[42] Y. J. Cortese, *et al.*, "Review of catheter-associated urinary tract infections and in vitro urinary tract models," *J. Healthcare Eng.*, vol. 2018, pp. 1–16, 2018.
[43] S. M. Jacobsen, *et al.*, "Complicated catheter-associated urinary tract infections due to escherichia coli and proteus mirabilis," *Clin. Microbiol. Rev.*, vol. 21, no. 1, pp. 26–59, 2008.
[44] A. Balcht and S. Raymond, "Pseudomonas aeruginosa: Infections and treatment," *Inf. Heal. Care.*, vol. 12, pp. 83–84, 1994.
[45] H. Fujikawa, A. Kai, and S. Morozumi, "A new logistic model for Escherichia coli growth at constant and dynamic temperatures," *Food Microbiol,* vol. 21, no. 5, pp. 501–509, 2004.
[46] J. Paredes, S. Becerro, and S. Arana, "Label-free interdigitated microelectrode based biosensors for bacterial biofilm growth monitoring using Petri dishes," *J. Microbiol. Methods*, vol. 100, no. 1, pp. 77–83, 2014.
[47] T. Wang, *et al.*, "Accumulation mechanism of biofilm under different water shear forces along the networked pipelines in a drip irrigation system," *Sci. Rep.*, vol. 10, no. 1, pp. 1–13, 2020.